

## INFLUENCE OF THE BLADE COUNT RATIO ON AERODYNAMIC FORCING PART II: HIGH PRESSURE TRANSONIC TURBINE

**Florian Fruth**

Royal Institute of Technology  
Heat and Power Technology  
S-100 44 Stockholm, Sweden

**Damian M. Vogt**

Royal Institute of Technology  
Heat and Power Technology  
S-100 44 Stockholm, Sweden

**Torsten H. Fransson**

Royal Institute of Technology  
Heat and Power Technology  
S-100 44 Stockholm, Sweden

### ABSTRACT

*The influence of the Blade Count Ratio (BCR) on the aerodynamic forcing of a transonic high pressure turbine has been investigated numerically. Main focus here was put on the change in unsteady aerodynamics, modal properties and the mode excitation. Using a scaling technique, six different transonic turbine stages with different numbers of scaled blades but maintained steady aerodynamics were generated and further analyzed. In the analysis a non-linear, time marching CFD solver was used and the unsteady, harmonic forces projected onto the mode shapes. For this transonic turbine the unsteady pressure at the rotor blade decreases in amplitude and spanwise distribution from low to high blade count ratios. In chordwise direction a local minimum for intermediate blade count ratios was found for the rotor and stator blades. Mode frequencies decreased monotonically with an increasing BCR. Significant mode changes for modes 5 and 6 of the different BCRs were captured using the Modal Assurance Criteria. It was found that for these transonic turbines the blade count ratio and reduced frequency are amongst others key parameters for a reduction in aerodynamic forcing. Even though an almost monotonic trend was found for the stator blade excitation, the rotor blade excitation behaves highly non-monotonic. A maximum value in excitation potential was found close to reported blade count ratio values. Optimization of certain modes is possible but case dependent, due to the non-monotonic nature. Moreover it was found that for a minor increase in upstream blade count the mean unsteady forces on the rotor blades is reduced, but the mode excitation not necessarily has to decrease.*

### 1 INTRODUCTION

In the development of gas turbines nowadays, forced response and flutter have become an important topic, due to lighter and slimmer blade designs. This change in shape leads to a reduction of the blade eigenfrequencies. When determining the integrity of a turbomachine, the frequency is of high interest, as components with low natural frequencies are more prone to lead to vibration problems and fatigue. Beside the eigenfrequencies, the mode shape changes also have a strong influence on the final forcing. Although forced response problems are considered in the development process, the blade shapes are mainly optimized for performance.

In order to reduce the unsteady forcing on blades, the sources of excitation as well as possibilities to reduce the forces have been investigated. Neglecting blade profile changes, modifications that can be made to reduce the unsteady forcing can be summarized as follows:

- Axial Gap
- Clocking
- Blade Count Ratio BCR (Downstream/Upstream)

Even though the unsteady forces can be reduced with these methods, the overall excitation of certain mode shapes is not necessarily reduced. This is due to the movement of the location of the highest unsteady forces on the blade surface and the phase shift between the different excitation sources, both of which can have a beneficial but also negative impact on the excitation of certain modes. The axial gap method generally uses the exponential decay of the potential field, but has a rather low

impact on the wake strength and shock wave. With the clocking method mainly the phase between the excitation sources can be controlled and optimized.

In contrast, increasing the blade count of the upstream row leads to a more homogeneous distribution of the unsteady forces on the blade surface [1], with an overall lower average forcing on the blades. For a 2D potential flow, Rao found the optimum to be  $BCR = 1.00$  [2]. Further investigations by Sokolowskij and Gnesin showed a maximum unsteady force for the equivalent of  $BCR = 3.33 - 4.00$  and a minimum for  $BCR = 0.83$  in 2D non-viscous simulations [3]. Gallus summarized the experimental and numerical findings of several investigations on the pitch ratio, the inverse of the blade count ratio, and concluded that the stimulus drops with an increasing number of upstream blades [4]. He points out that for an overall favorable blade count, the blade vibration characteristics, and all components of the turbomachine have to be considered, i.e. the blades, disks and the shaft. His investigation also examined the influence on aeroacoustics, and it was found that a large frequency range of damped sound pressure can be achieved, when the blade count of the adjacent rows has a high difference. Even though the highly different blade count produces a much higher sound pressure level than the other ones, the sound is damped out much faster due to the cut-off frequency. This leads to opposite requirements for low unsteady forcing and aeroacoustics [4].

More recent investigations on 3D transonic turbomachines were conducted by Rzadkowski et al.. They found that the unsteady loads of blades but also the modal force amplitudes can be reduced by choosing a high number of upstream stator blades [5]. By increasing the number of upstream blades, the average and harmonic forces are reduced but they pointed out the efficiency of the stage tends to go down at the same time [1]. Due to the low number of cases, Rzadkowski et al. were not able to find an overall describing relation between the unsteady forces and the blade count ratio. A previous investigation by the authors [6] on a transonic compressor gives a detailed comparison of nine different blade count ratios, their influence on the unsteady flow as well as on the excitation of modes shapes. The trend of overall lower unsteady forces for a higher number of upstream blades was also found, but it was shown that this has the opposite effect on the upstream blade row. It was also pointed out, that a minor change in blade count ratio can lead to a significant change in mode excitation, and that the relation between the blade count ratio and the excitation of modes is of a non-monotonic nature.

The objective of this investigation is to extend the previous numerical investigation by Fruth et al. to a transonic turbine. Due to much stiffer turbine blades and different flow conditions, the relative relation between the BCR and the aerodynamic forcing differs from the compressor results.

## NOMENCLATURE

### Symbols

$A$	Mode Displacement	[m]
$B$	Blades	[-]
$P$	Pressure Side	
$N$	Node Number	[-]
$S$	Suction Side	
$SF$	Scaling Factor	[-]
$TP$	Period between two Excitations	[s]
$U$	Flow Velocity	[m/s]
$c$	Chord Length	[m]
$dx, dy, dz$	Mode displacements	[m]
$f$	Frequency	[1/s]
$k$	Reduced Frequency	[-]
$p$	Pressure	[KPa]
$\tilde{p}$	Normalized Unsteady Pressure	[-]
$\bar{p}$	Average Pressure	[KPa]
$t$	Time	[s]
$\omega$	Rotational Speed	[rpm]

### Subscripts

$ax$	Axial
$f$	Subscript for Rotor or Stator
$g$	Generalized
$max$	Maximum
$n$	Node
$norm$	Normalized
$orig$	Original
$sca$	Scaled
$xyz$	Euklidean norm of dx, dy, dz
0	Total
1	Inlet

### Abbreviations

BCR	Blade Count Ratio (Downstream/Upstream)
CFD	Computational Fluid Dynamics
FEM	Finite Element Method
HCF	High Cycle Fatigue
LE	Leading Edge
MAC	Modal Assurance Criteria
RF	Reduced Frequency
TE	Trailing Edge

## 2 METHODS

### 2.1 Method to Investigate the Influences of the Blade Count Ratio

As in the previous investigation on the transonic compressor by Fruth et al. [6], the following aspects are addressed when changing the blade count ratio:

1. Change in unsteady flow
2. Change in modal properties
3. Change in modal excitation
4. Change in the Campbell diagram

Here the steady state solution of the original blade count ratio is used to generate new turbine geometries with different blade count ratios and initial solutions, by scaling both. When scaling, solidity is maintained leading to a comparable steady flow. Further information on the scaling technique can be found in chapter 2.3. For all the different blade count ratio cases, unsteady flow simulations are conducted.

The change in unsteady flow is then analyzed by space time plots, giving the normalized, unsteady pressure distribution both along the chord and through time.

Due to the different size of the rotor blades the modal properties change. These changes are examined by looking at the frequency change and the Modal Assurance Criteria (MAC). The MAC number is a single value on the agreement of two different shapes, in this case comparing the displacements with the ones of the highest BCR=3.00 in each node. The Euclidean norm of the nodal displacements in all three coordinate directions  $A_{xyz}$  is used to define the MAC number as follows:

$$MAC = \frac{|A_{xyz,i}^T A_{xyz,j}|^2}{(A_{xyz,i}^T A_{xyz,i}) (A_{xyz,j}^T A_{xyz,j})} \quad (1)$$

In the case where the mode shapes are the same the MAC number is one, whereas it is zero for completely different mode shapes.

The modal excitation is calculated in a decoupled manner, with a projection of the aerodynamic forces onto the mode shapes of the respective blade count ratio. Additionally it is investigated in how far the modal excitation changes for one specific BCR, using different stator blade counts. The generalized force is here used as a measure to compare the different modal excitations, looking at the first six modes.

These modal excitations are also related to the reduced frequency, which is a more flow relevant parameter, as it describes the time for a particle to cross the chord ( $t_c$ ) divided by the period of one blade oscillation ( $TP$ ).

$$k = \frac{t_c}{TP} = \frac{f \cdot c_{ax} \cdot SF_f}{U_{ax}} \quad (2)$$

For this investigation, using the same steady state solution, only the axial chord  $c_{ax}$ , the scaling factor  $SF_f$  of the row and the oscillation frequency  $f$  change. The scaling factor  $SF_f$  is furthermore described in chapter 2.3. Overall, the reduced frequency gives an indication of the amount of perturbation sources between two blades and their chords when running under these flow conditions. Having the same mass flow in this investigation, a higher reduced frequency means more perturbations, but smaller in magnitude.

## 2.2 Computational Approach

In this investigation the fluid-structure interaction is calculated using an uncoupled method, leading to the forced response analysis. This means that the CFD simulation is conducted once for each case of blade count ratio, separately from the modal analysis. The aerodynamic forces from the CFD simulation are Fourier-transformed afterwards to get the harmonic content. These forces are mapped onto a FEM mesh and overlaid with the results of the modal analysis, i.e. the mode shapes and frequencies.

The CFD calculations are conducted with the in-house solver VOLSOL, with methods being explained in [7,8]. In this investigation the 3D viscous, compressible and non-linear Navier-Stokes solver is chosen with a k-ε turbulence model. Convective fluxes are calculated with a third order upwind scheme, whereas a second order central scheme is used for the viscous fluxes. Furthermore a three stage Runge-Kutta scheme, of second order accuracy, is employed for time discretization. Convergence of the solution is checked upon the relative magnitude difference of two consecutive maximums of the periodic tangential forces, and was considered to be converged when less than 0.05%.

Specific to this investigation, adiabatic walls are modeled with the non-slip condition and employing the law of wall for a correction of the friction at unresolved boundary layers. Inlet and outlet boundary conditions are modeled with mixed pressure boundary conditions, with an additional radial equilibrium equation for the outlet to define the static pressure. Depending on the local flow condition i.e. subsonic or supersonic, the inflow and outflow conditions are adjusted automatically. The rotor-stator interface is modeled with a simple rotational sliding interface using overlapping ghost cell layers and a non-reduced number of passages simulated. Data exchange over the interface is performed using a zero order search [9].

For the modal analysis commercial software (ANSYS 11.0) and the in-house post-processor AROMA (Aeroelastic Reduced Order Model Analysis [10]) are applied. Using the stiffness and mass matrices from ANSYS, the mode shapes and mode frequencies are calculated by AROMA as well as the final projection of the aerodynamic forces onto the mode shapes.

## 2.3 Scaling Method

In general the scaling method is used to reduce calculation time, by calculating only a sector of the scaled geometry. It generates new, scaled geometries which are circumferentially periodic and have comparable steady aerodynamics. This is achieved by maintaining solidity, the pitch-to-throat ratio and the blade inlet metal angles. Using the scaling method, the rotor and stator blades are scaled separately with a scaling factor  $SF$ . This scal-

ing factor is calculated using the number of blades in the original case  $\#B_{orig}$  and the number of scaled blades  $\#B_{sca}$ :

$$SF_f = \frac{\#B_{orig}}{\#B_{sca}} \quad (3)$$

This leads to a scaling factor for the rotor  $SF_r$  and stator  $SF_s$ . The method itself is described more in detail e.g. by Mayorca et al. [11], Schmitz et al. [12] and Clark et al. [13] including the influence of this reduction method on the accuracy of the calculations. In this study, the scaling method is used intentionally to create turbines with a different blade count ratio.

The axial gap is kept almost constant in the code and varies from -3.3% to +5.9% of the original gap size, increasing for lower blade count ratios. This is compensating for the size change of the rotor potential field. Including the change in chord, the gap-to-chord ratio varies from a value of 0.40 to 0.88 from low to high BCRs, which can be related to the rotor wake decay and the size of the rotor potential field. As the process of wake decay is rather slow, the difference for small axial gaps is clearly outweighed by the change of the chord due to the scaling.

## 2.4 Generalized Forces

The influence of the different blade count ratios on the aerodynamic forcing of the rotor and stator blades is described by the non-dimensional generalized force. It describes how structural modes are excited by the fluid forces for a certain harmonic. In order to conserve the overall integrated forces on the blades, the forces obtained from the CFD mesh are mapped onto the corresponding FEM mesh. Blade motion and its influence on the unsteady pressure is not modeled in this investigation.

As a first step, the real and imaginary parts of the harmonic forces are calculated from the time-marching CFD results using a Fourier transformation. Using the real and complex force components, the generalized forces for both are calculated by a projection of the forces onto the mode shapes (see Eq. 4, 5), which are normalized by the maximum mode amplitude  $A_{max}$

$$F_{g,cos} = \frac{\sum_{n=1}^N F_{x,cos,n} \cdot dx_n + F_{y,cos,n} \cdot dy_n + F_{z,cos,n} \cdot dz_n}{A_{max}} \quad (4)$$

$$F_{g,sin} = \frac{\sum_{n=1}^N F_{x,sin,n} \cdot dx_n + F_{y,sin,n} \cdot dy_n + F_{z,sin,n} \cdot dz_n}{A_{max}} \quad (5)$$

The final generalized force contains the phase and amplitude as described by Eq. 6 and is normalized by the average tangential force as in Eq. 7.

$$F_g = \sqrt{F_{g,cos}^2 + F_{g,sin}^2} \quad (6)$$

$$F_{g,norm} = \frac{F_g}{F_t} \quad (7)$$

In order to compensate for the different speed at which the crossings appear the following approximation is used to scale the generalized forces for all results. It is exact for subsonic cases and can be derived from basic turbomachinery laws:

$$F_{comp} = \left( \frac{\omega_{act}}{\omega_{cfd}} \right)^2 \cdot F_{g,norm} \quad (8)$$

## 3 NUMERICAL TEST CASES

For this investigation the BRITE high pressure, transonic turbine stage MT1 is used, which has been installed in the Pyestock Light Piston Facility by Hilditch et al. [14]. Numerical simulations have been conducted on this stage by Laumert et al. for investigations on blade excitation mechanisms [15]. The nominal operating conditions of the MT1 turbine stage, from now on called DERA, can be found in Table 1 along with the values chosen for the numerical investigation.

Table 1. TURBINE DATA AT NOMINAL SPEED AND CHOSEN SIMULATION SETTING

Parameter	Nominal	Simulation
Mass Flow [kg/s]	17.25	16.98-17.01
Pressure Ratio	0.31	0.31
Shaft Speed [rpm]	9500	9500
Stator Blade Count	32	32
Rotor Blade Count	60	48-96

The investigated range of blade count ratio is from 1.25 to 3.00 with six different cases to study, with the blade count ratio of the original transonic turbine being 1.88. A detailed description of the cases can be found in Table 2.

In order to reduce the number of possible influences on the flow field, the number of stator blades is kept constant at 32, whereas the number of rotor blade is varied from 40 to 96. For these flow conditions, the reduced frequencies for the stator blades range from 4.67 to 11.21 and for the rotor blades from 0.85 to 2.03.

The CFD mesh used in this investigation (see Figure 1) is block structured and refined based on that used in the investigation of Laumert et al. [8], using O-grids for the blade profiles, H-grids for the other blocks, and an overall node number of 481108. It has 41 nodes in the radial direction with 5 nodes

Table 2. DIFFERENT CASES USED FOR BCR STUDY

Case	BC	BCR	S <sub>s</sub>	S <sub>r</sub>	k <sub>s</sub>	k <sub>r</sub>
S4R5	S32R40	1.25	1.00	1.50	4.67	2.03
S2R3	S32R48	1.50	1.00	1.25	5.61	1.69
S4R7	S32R56	1.75	1.00	1.07	6.54	1.44
S2R4	S32R64	2.00	1.00	0.94	7.48	1.27
S2R5	S32R80	2.50	1.00	0.75	9.35	1.01
S1R3	S32R96	3.00	1.00	0.63	11.21	0.85

for the tip clearance, 9 nodes for the rotor and 12 nodes for the stator O-grid respectively.

The Finite Element meshes for rotor and stator blades use brick elements (ANSYS Element 45) and are refined at the leading-, trailing edge and also at hub and tip, with 7000 nodes for the stator and 5000 nodes for the rotor blades. It was found in a pre-study that the eigenfrequencies converge already for a lower number of nodes.

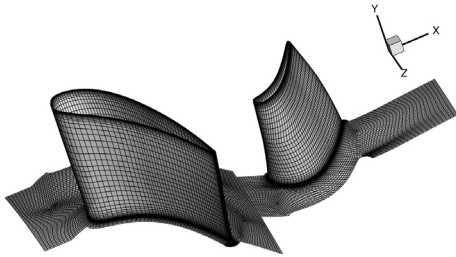


Figure 1. CFD MESH OF TRANSONIC TURBINE DERA

## 4 RESULTS

### 4.1 Steady State

The steady state result of the DERA case shows a fully choked stator blade starting from the pressure side mid chord to the trailing edge of the suction side of the next blade, covering the complete span.

In order to be able to compare the different blade count geometries, the steady aerodynamics has to be maintained. Looking at Figure 2 which shows the loading of the stator and rotor blades at 90% span, i.e. the normalized, time-averaged pressure, the requirement is fulfilled. This is also the case for the other span positions. The different loadings agree very well, and only

from 70-90% chord position on the suction side of the rotor and stator blade, minor differences can be seen. Due to the high similarity of the different transonic turbines a comparison of the further unsteady aerodynamics and forcing is sound.

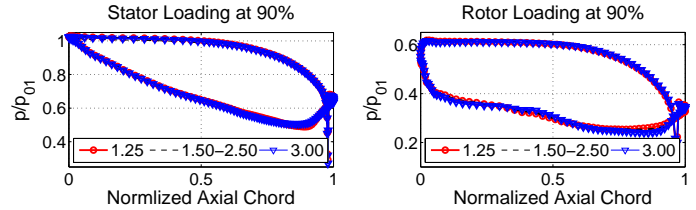


Figure 2. COMPARISON OF STATOR (LEFT) AND ROTOR BLADE LOADINGS (RIGHT) FOR DIFFERENT BCRs

### 4.2 Modal Properties

When scaling the blades to generate a new turbine with different blade count ratios, the blade shapes are scaled in the axial and circumferential directions, leading to different structural behavior. Of main interest here are the changes in mode frequency and mode shape, which can be found in Figure 3.

What can be seen, for the rotor blades giving similar steady aerodynamics, is an almost linear decrease in mode frequencies for modes 1-4 from low blade count ratio to high blade count ratio. Higher blade count ratio means a shorter axial chord and a lower profile thickness, which is generally less stiff and therefore has lower mode frequencies. For higher modes such as mode 5 and 6, this monotonic trend is not the case.

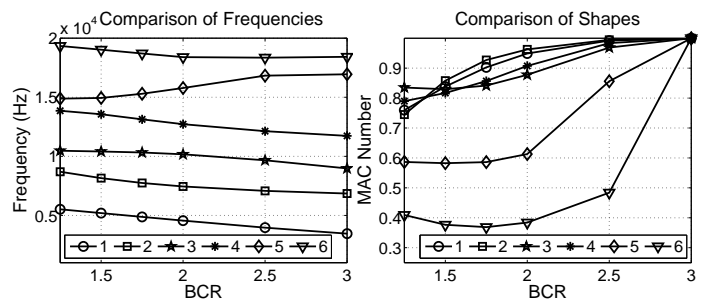


Figure 3. COMPARISON OF MODE FREQUENCIES (LEFT) AND MODE SHAPES USING MAC NUMBER (RIGHT, RELATIVE TO BCR=3.00)

The reason for this can be seen when comparing the mode shapes 1-6 by using the MAC number. The MAC numbers are

also presented in Figure 3, and all shapes are compared to the mode shapes of the highest blade count ratio to see the trends for an increasing BCR. As already seen in the mode frequency behavior, the mode shapes for mode 1-4 are in general very similar and thus have a high MAC number. This is not the case for modes 5 and 6, and explains the differences in the mode frequencies. Due to a rather different mode shape, the according mode frequencies do not align with the ones from mode 1 to 4.

### 4.3 Change in Unsteady Flow

Even though the overall loading of the different transonic turbines does not change, i.e. the time averaged pressure distribution, the normalized unsteady pressure distribution changes highly as could already be seen in the previous investigation of the authors. In order to compare the different flow fields, the space time plots are used, which show the following normalized unsteady pressure over two periods (abscissa) along the chord (ordinate):

$$\tilde{p} = \frac{p - \bar{p}}{p_{01}} \quad (9)$$

The different space time plots of the stator blades show a similar flow field concerning the pressure distribution (see Figure 4 left). A difference that can be seen is that for lower blade count ratios high unsteady pressure spreads further from trailing edge (TE) to leading edge (LE). The higher normalized pressure for BCRs 1.25 until BCR 1.75 can be explained by the relatively bigger rotor blades downstream that have a bigger potential field at their TE and outweigh the change in axial gap. Nevertheless this trend towards lower unsteady pressure for higher BCRs is not monotonous, which will furthermore be examined in the discussion section.

Looking at the rotor blade space time plots (see Figure 4 right), a distinct difference can be seen in their flow field, but comparing the lower (BCR 1.25 and 1.50), middle (BCR 1.75 and 2.00) and upper (BCR 2.50 and 3.00) blade count ratio cases, similarities can be found. When comparing these three different groups a change in pressure magnitude, phase and chord position can be seen. As it was the case for the stator blades, also the pressure magnitude of the rotor blades does not change monotonically.

The unsteady aerodynamics of both stator and rotor blades show up a local minimum in unsteady pressure and therefore forcing, which has a significant influence on the overall excitation of the modes.

In the blade-to-blade view in Figure 5, showing the 90% span position, the significant and local unsteady pressure seen in the space time plot at the rotor leading edge of BCR=1.25 can be confirmed. Furthermore also the broad unsteady pressure distribution at the pressure side of BCR=3.00 is found. The dense

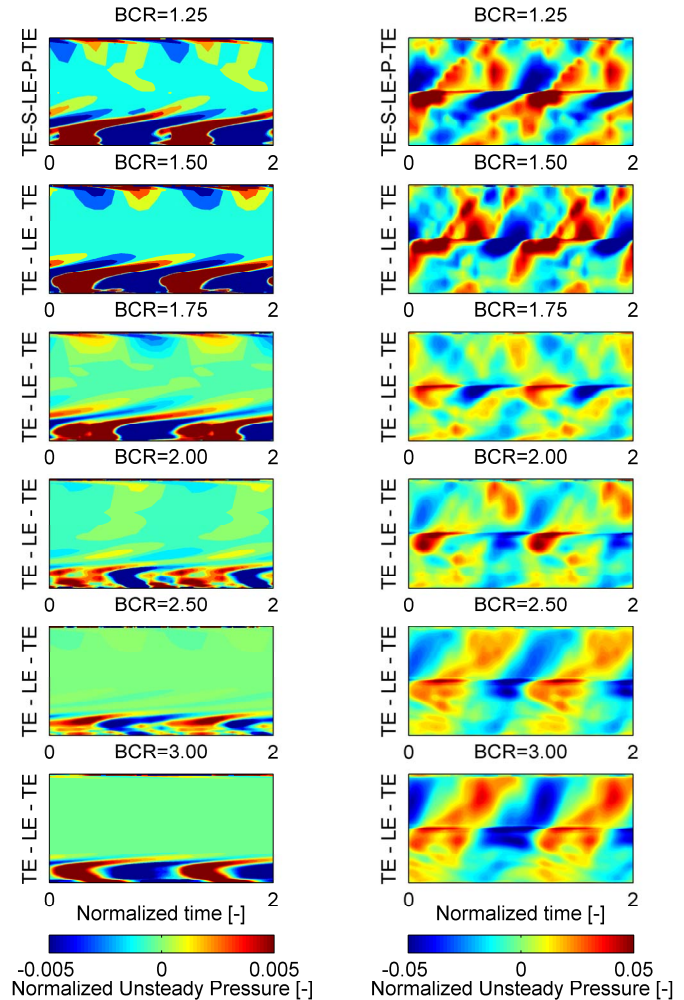


Figure 4. COMPARISON OF STATOR (LEFT) AND ROTOR BLADE (RIGHT) SPACE TIME PLOTS OF NORMALIZED UNSTEADY PRESSURE AT 90% SPAN

circumferential distribution of rotor blades for BCR=3.00 obviously leads to a blockage and a rather high back-pressure. Due to the comparatively significant potential field of the rotor leading edge of BCR=1.25, the stator trailing edge is exposed to high unsteady pressure fluctuations at the suction and pressure side.

### 4.4 Influence of the Change in Unsteady Flow and Mode Shape on Forcing

When projecting the unsteady aerodynamic forces onto the mode shapes, the overall excitation of the mode shapes can be quantified with the generalized force. Due to a change in unsteady flow and a slight change in mode shape, the overall excitation does not have to follow necessarily the trends of the pressure magnitudes in the space time plots.

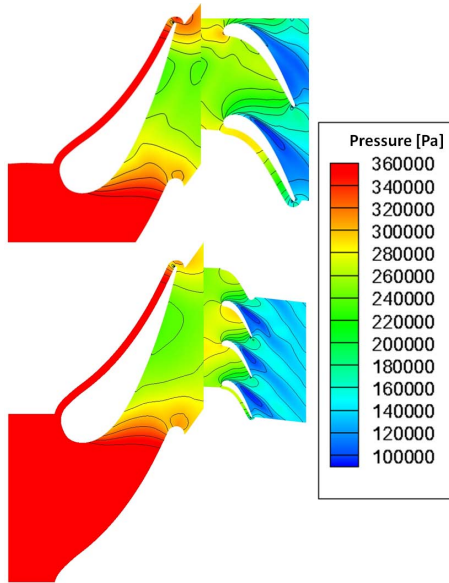


Figure 5. COMPARISON OF BLADE-TO-BLADE PRESSURE DISTRIBUTION AT 90% SPAN BETWEEN BCR=1.25 (TOP) AND BCR=3.00 (BOTTOM)

**4.4.1 Stator** An overview of the influence of the blade count ratio on the stator blade forcing can be found in Figure 6.

A clear trend for the stator blades and all modes can be seen with higher generalized forces for lower blade count ratios, i.e. bigger downstream rotor blades. This can be related to the six mode shapes, which are all dominated by TE deflections. Even though the axial gap is slightly increased for lower blade count ratios to compensate for the growing potential field of the rotor blades downstream, the potential field is dominant.

The relatively high generalized forces of the modes 3, 4 and 5 can be explained with their mode shapes, as they also have deflections, i.e. forcing sensitive zones, between the TE and mid chord. Having high unsteady pressure and forces in these regions, as could be seen in the space time plots, leads to these overall high generalized forces.

**4.4.2 Rotor** The influence of the blade count ratio on the rotor blade modes can be found in Figure 7. In contrast to the stator forcing no general trend is prevalent.

Here, only mode 1 has a monotonic increase in generalized forces for increasing BCR. This can be associated with the change in mode shape, i.e. the steady movement of the sensitive tip region from trailing edge to leading edge for the different

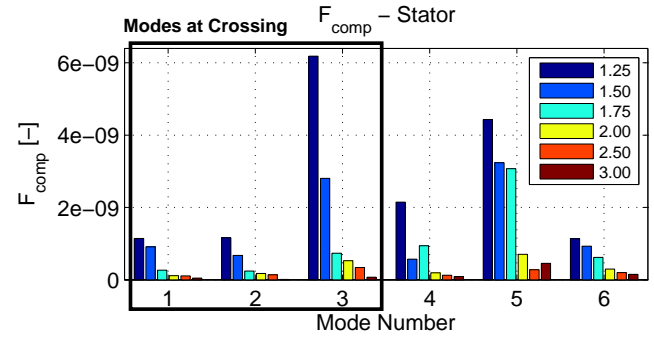


Figure 6. GENERALIZED FORCES FOR DIFFERENT BCRs OF THE STATOR FOR FIRST HARMONIC, MODES 1-6

blade count ratios. Therefore BCR=3.00 is more susceptible to high unsteady forces at the LE than BCR=1.25.

Modes 2, 3, 4 and 6 reveal a common pattern (with minor exceptions), where the generalized forces decrease at first before increasing again from BCR 1.75/2.00 on. Due to the rather high difference in mode shape (especially mode 6), this common pattern has to be associated with the unsteady aerodynamics, which shows up a similar behavior.

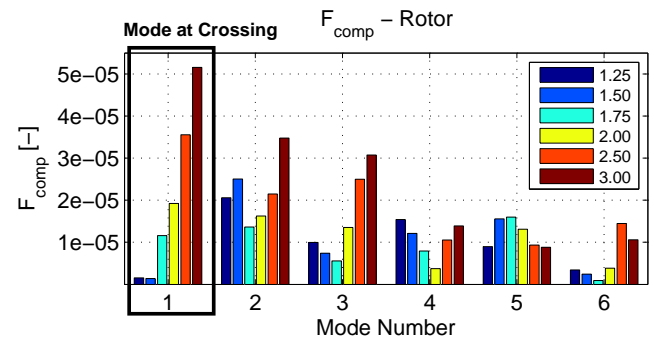


Figure 7. GENERALIZED FORCES FOR DIFFERENT BCRs OF THE ROTOR FOR FIRST HARMONIC, MODES 1-6

## 4.5 Influence of the Reduced Frequency on Forcing

A more flow based parameter than the blade count ratio is the reduced frequency for which all the generalized forces are presented in Figure 8.

It can be seen for the rotor and stator blade that a higher reduced frequency leads to a lower forcing for most of the cases.

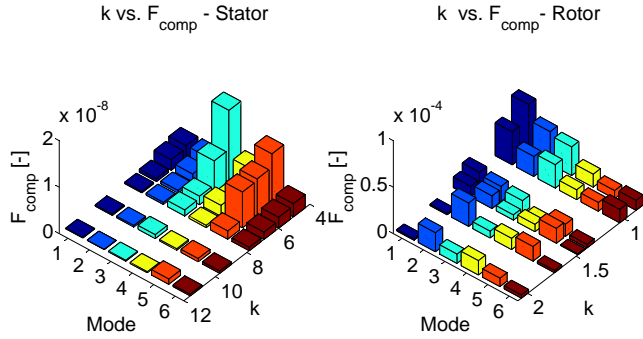


Figure 8. INFLUENCE OF REDUCED FREQUENCY ( $k$ ) AND MODE ON GENERALIZED FORCES ( $F_{comp}$ )

In general the reduced frequency describes the number of perturbations in a blade passage at every instant. The results for generalized forces show that it is preferable to have more, small perturbations. As a low RF for the stator blade means a high RF for the rotor blades, a reduced frequency in the mid range has to be chosen to optimize the overall stage for resonance occurrence.

#### 4.6 Influence of the Blade Count on Forcing for same Blade Count Ratio

The parameter blade count ratio is of a relative nature, meaning that it can be achieved with various rotor-stator blade count combinations. Assuming only minor changes of blade count in practice, the influence of the stator blade count from 30-34 on aerodynamic forcing with the same BCR=2.00 is furthermore examined.

For the six modes examined (see Figure 9), it can be seen that the BCR is not the only important parameter as the generalized forces vary already for minor changes in stator blade count. The variation has a trend towards lower generalized forces for a higher stator blade count, but does not apply for all modes.

Looking at the space time plots in Figure 9, a clear decrease in unsteady pressure fluctuations is present, as outlined by Rzadkowski and Soliński [1] and Gallus et. al [4]. This is also confirmed by the harmonic integrated forces for the three cases, decreasing from 21.5N to 18.0N for higher upstream blade count. But minor differences can be seen in the pressure distribution that can lead to a different trend in mode excitation, as e.g. seen for mode 4 and 6, when projecting the forces onto the mode shapes.

For a major increase in upstream blade count the unsteady forcing and mode excitations decrease, as report by [1,4]. This

decrease in unsteady forces can also be seen for a minor increase in blade count as seen from the harmonic integrated forces. But when looking at mode excitation, the influence of the modal properties, pressure distribution and phase is comparatively of high importance and can lead to an increase in generalized forces.

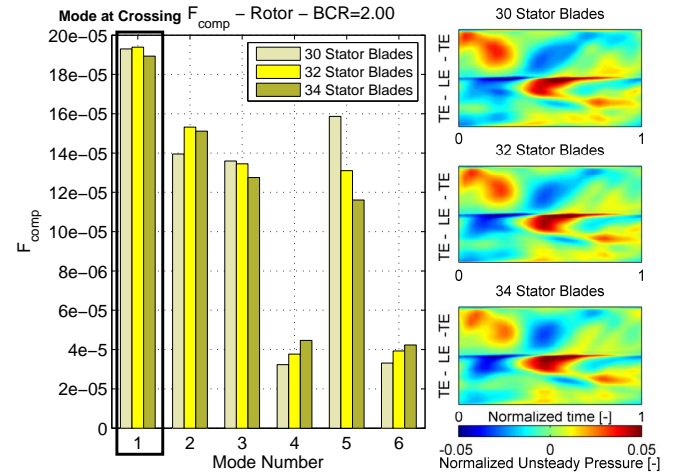


Figure 9. INFLUENCE OF THE STATOR BLADE COUNT FOR CONSTANT BCR (LEFT) AND SPACE TIME PLOTS (RIGHT)

## 5 DISCUSSION

### 5.1 Applicability of the Blade Count Ratio

It has been shown in [6] for a transonic compressor that the change in blade count ratio has opposite effects on rotor and stator rows, related to the excitation, but that an overall optimization leads to a significant reduction of the aerodynamic forcing. This can also be confirmed for this transonic turbine, which shows a maximum increase in generalized forces for a mode by 1074.2%, using BCR 2.0 as the reference value. An overview of minimum and maximum changes can be found in Table 3. These changes refer to the broad range of blade count ratios chosen.

The BCR variation leads to two major changes in the Campbell diagram when comparing the results, which are in the case of a constant stator blade count:

1. Multiple exciting engine orders for stator blades due to different rotor count
2. Multiple mode frequencies for a mode due to different rotor blade sizes

Allowing only reasonable, minor changes of 15% in the rotor blade count, the critical rotor mode 1 is furthermore ana-

lyzed in the Campbell diagram (see Figure 10). Eigenfrequencies in this diagram are calculated using the centrifugal forces at 9500rpm. The size of the circles is representative for the magnitude of generalized forces, with a cross for very small values.

Table 3. OVERVIEW OF MAXIMUM INCREASE AND REDUCTION OF  $F_{comp}$  COMPARED TO BCR 2.00

	Reduction of $F_{comp}$	Increase of $F_{comp}$
<b>Stator</b>	-93.0% (Mode 2)	+1074.2% (Mode 3)
<b>Rotor</b>	-92.8% (Mode 1)	+275.8% (Mode 6)

In order to decrease the forcing of the critical mode 1 from the reference value of BCR=2.00, the blade count ratio has to be decreased, meaning here changing to BCR=1.75. This leads to a reduction in generalized force by 39.6%, but the crossing is at 9145 rpm compared to 8550 rpm before, and therefore closer to the operating speed of 9500 rpm.

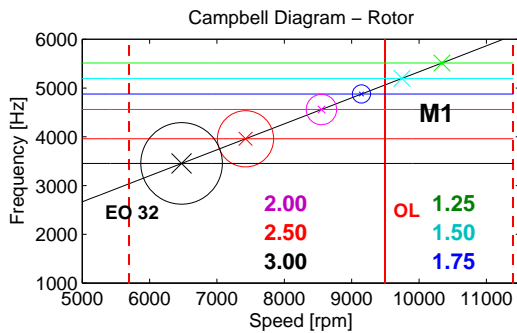


Figure 10. CAMPBELL DIAGRAM FOR ROTOR BLADE MODE 1 AND DIFFERENT BLADE COUNT RATIOS

Using the blade count ratio the excitation potential of a critical mode in the rotor row could be decreased. A further optimization between the rotor row and stator row can lead to an overall reduced HCF risk.

Overall a non-linear change in excitation potential by one order of magnitude was found, where already minor changes in BCR can lead to a significant increase or decrease in forcing. Similar to Rzadkowski et al. [1] which found the maximum forcing for the equivalent of  $BCR = 3.33 - 4.00$ , the maximum on the rotor blades was found for  $BCR = 3.00$ , representing the

highest blade count ratio in this investigation. Due to the rather low axial gaps, the exponential decay of the potential fields is not influential in comparison to the change in potential field.

The BCR can be used for a global optimization of the aerodynamic forcing, due its significant, non-linear variation in generalized forces, but is case dependent. Keeping the BCR constant, it was shown that the blade count has an influence on the mode excitation, which is for minor blade count changes not necessarily monotonic. Another method, which is not further elaborated in this investigation, is the simple change in blade count to suppress undesired excitation frequencies.

## 5.2 Change in Unsteady Aerodynamics

Due to the significant influence of the unsteady aerodynamics in the excitation of the rotor blades, the changes of unsteady aerodynamics related to the BCRs are furthermore elaborated. Regions of high interest are the leading edge as, it is directly exposed to the excitation sources generated by the stator blades, and furthermore the trailing edge where most of the considered modes have high deflections. A comparison of the spanwise leading edge space time plots can be found in Figure 11 and the trailing edge plots in Figure 12. For LE and TE the same time period is chosen, and values taken from a single line of nodes along the span at minimum and respectively maximum axial blade position.

The leading edge plots show a good agreement for the different BCR cases, meaning that the overall unsteady pressure field does not change significantly. Nevertheless minor differences can be found related to the magnitude of unsteady pressure and the distribution. BCRs 1.25 and 1.50 have larger zones of high unsteady pressure and differences can be found in the distribution at the hub and tip section. For low BCRs both are exposed a similar time period to high unsteady pressure, whereas for the high BCRs the region between hub and mid span are exposed to high unsteady pressure for a longer time period than the tip with an overall lower magnitude.

Looking at the trailing edge, the distribution of the unsteady pressure varies significantly and is highly localized for the higher BCRs in the section between hub and mid span. As the mode shapes have high deflections along the complete trailing edge span, this change in distribution leads to an overall higher excitation for low BCRs, which could be seen in Figure 12 and explains the significant changes.

Not only the pressure distribution along the span changes, but also the magnitudes. The maximum unsteady pressure amplitudes along the span for the different BCRs are compared in Figure 13. At the LE a significant decrease in maximum pres-

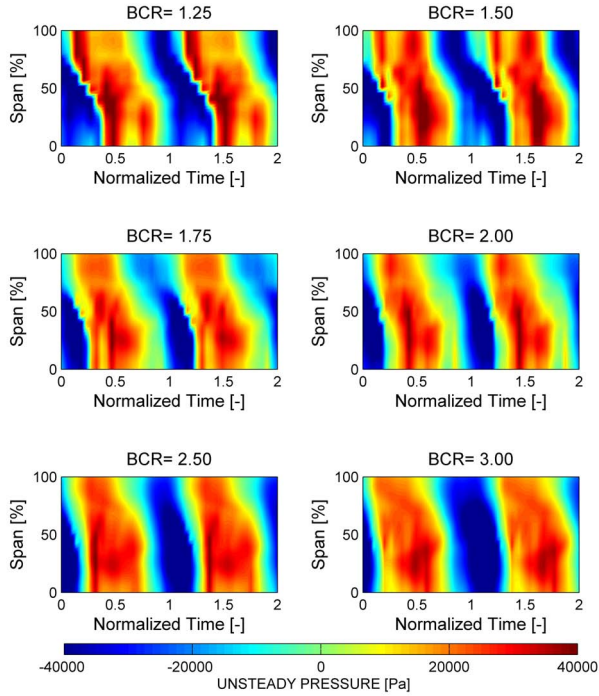


Figure 11. SPANWISE SPACE TIME PLOT OF UNSTEADY PRESSURE AT LE

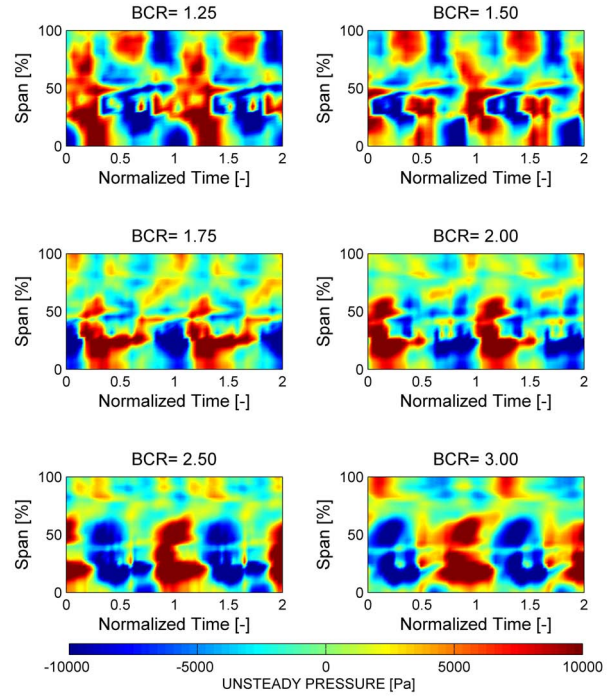


Figure 12. SPANWISE SPACE TIME PLOT OF UNSTEADY PRESSURE AT TE

sure amplitude can be seen from low to high BCRs. Furthermore the low BCRs have high unsteady pressure values along the complete span that become more localized at 30% span position for high BCRs. In comparison to that, the maximum unsteady pressure at the TE can be found at 20-30% span for all BCRs with a slightly broader distribution for low BCRs.

## 6 CONCLUSION

In order to investigate the influence of the BCR on the aerodynamic forcing, six different transonic turbines were generated in the blade count ratio range of 1.25-3.00 having similar steady aerodynamics.

For the different blade count ratios analyzed, the mode frequencies change in an almost monotonic manner, except when the mode shape changes significantly. Additionally it could be seen using the MAC number, that the lower the modes, the more similar they are for different blade count ratios.

It was shown that the change in excitation for different BCRs is highly non-monotonic for the rotor blades but almost monotonic for the stator blades of this transonic turbine, and depends on the unsteady forces, phasing and mode shapes. Due to the complex interaction of these factors, no general

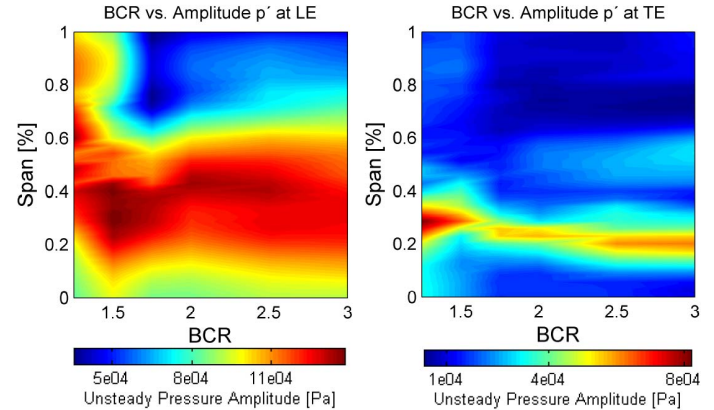


Figure 13. INFLUENCE OF BCR ON UNSTEADY PRESSURE AMPLITUDE AT LE (LEFT) AND TE (RIGHT)

conclusion can yet be drawn.

Furthermore it was pointed out that the blade count ratio is of a relative nature and that also the actual blade count has to be considered. For a major increase in upstream blade count the unsteady forces decrease as shown by others [1,4]. But for minor changes, with a lower change in forces, the influence of the modal properties, phase and pressure distribution can lead

for single modes to an increase in excitation.

The change in unsteady flow was analyzed and it was found that for lower BCRs the unsteady amplitudes are higher in magnitude and less localized in spanwise direction.

In a Campbell diagram for the rotor blades the potential use of the blade count ratio parameter for a single mode optimization was shown and a generalized force reduction of mode 1 by 39.6% achieved. The change in BCR leads amongst others to a movement of the crossings by moving the blade mode frequencies of one row, and to a change in the exciting engine order of the other row, assuming that one row is kept constant as it was done in this investigation.

An overall significant influence of the blade count ratio on the aerodynamic forcing was shown and analyzed for a transonic turbine and previously for a compressor. Low changes in reduced frequency or BCR can lead to a high decrease or increase in aerodynamic forcing. Hence an optimization of the forcing behavior is possible, but has influence on all modes and is case dependent due to the non-monotonic nature.

For a deeper understanding the local forcing minimum for similar BCRs of a compressor and turbine case has to be further investigated.

## ACKNOWLEDGMENT

The research has been funded by the Swedish Energy Agency, Siemens Industrial Turbomachinery AB and Volvo Aero Corporation through the Swedish research program TURBO POWER, the support of which is gratefully acknowledged.

## References

- [1] Rzadkowski R., Soliński M., "The Effect of Change in the Number of Stator Blades in the Stage on Unsteady Rotor Blade Forces", 5th International Conference on Vibration Engineering and Technology of Machinery, 2009, Wuhan, China
- [2] Rao J. S., "Turbomachine Unsteady Aerodynamics", Wiley Eastern Ltd., 1994, New Delhi, India
- [3] Sokolovskij G., Gnesin V., "Nonstationary transonic and viscous flow in Turbomachinery", Naukova Dumka, 1986, Kijev, Ukraine (in Russian)
- [4] Gallus H. E., Grollius H., Lampertz J., "The Influence of Blade Number Ratio and Blade Row Spacing on Axial-Flow Compressor Stator Blade Dynamic Load and Stage Sound Pressure Level", 81-GT-165, 1981
- [5] Rzadkowski R., Gnesin V., Kolodyazhnaya L., "The Influence of the Stator-Rotor Blade Number Ratio on the Aeroelastic behaviour of Rotor Blades", International Symposium on Dynamics of Steam and Gas Turbines, 2009, p. 213-224, Gdansk, Poland
- [6] Fruth F., Vogt D. M., Mårtensson H., Mayorca M. A., Fransson T. H., "Influence of the Blade Count Ratio on Aerodynamic Forcing Part I: Highly Loaded Transonic Compressor", GT2010-22756, ASME TurboExpo 2010
- [7] Eriksson L.-E., "Development and Validation of Highly Modular Flow Solver Versions in G2DFLOW and G3DFLOW Series for Compressible Viscous Reacting Flow", VAC Report 9970-1162 (Non-Public), Volvo Aero Corporation, Trollhättan, Sweden
- [8] Eriksson L.-E., "A Third Order Accurate Upwind-Biased Finite Volume Scheme for Unsteady Compressible Flow", VFA Report 9370-154 (Non-Public), Volvo Aero Corporation, Trollhättan, Sweden
- [9] Laumert B., Mårtensson H., Fransson T.H., "Simulation of Rotor/Stator Interaction with a 4D Finite Volume Method", GT-2002-30601, ASME TurboExpo 2002
- [10] Mayorca M. A., Fruth F., Vogt D. M., Fransson T. H., "Numerical Tool for the Prediction of Aeromechanical Phenomena in Gas Turbines", 15th Blade Mechanics Seminar, Winterthur, 2010
- [11] Mayorca M., De Andrade J., Vogt D., Mårtensson H., Fransson T. H., "Effect of Scaling of Blade Row Sectors on the Prediction of Aerodynamic Forcing in a Highly-Loaded Transonic Compressor Stage", GT2009-59601, ASME Turbo Expo 2009
- [12] Schmitz M. B., Schäfer O., Szwedowicz J., Secall-Wimmel T., Sommer T. P., "Axial Turbine Blade Vibrations Induced by the Stator Flow. Comparison of Calculations and Experiment", Unsteady Aerodynamics, Aeroacoustics and Aeroelasticity of Turbomachines, 2006, pp. 107-118
- [13] Clark J. P., Stetson G. M., Magge S. S., Ni R. H., Haldermann C. W., Dunn M. G., "The Effect of Airfoil Scaling on the Predicted Unsteady Loading on the Blade of a 1 and 1/2 Stage Transonic Turbine and a Comparison with Experimental Results", GT2000-0446, ASME Turbo Expo 2000
- [14] Hilditch M. A., Fowler A., Jones T. V., Chana K. S., Oldfield M. L. G., Ainsworth R. W., Hogg S. I., Anderson S. J., Smith G.S. "Installation of a turbine stage in the Pyestock Isentropic Light Piston Facility", 94-GT-277, 1994
- [15] Laumert B., Mårtensson H., Fransson T.H., "Investigation of Unsteady Aerodynamic Blade Excitation Mechanism in Transonic Turbine Stages", GT-2002-30450, ASME TurboExpo 2002

# Appendix

## Mode Shapes - Stator

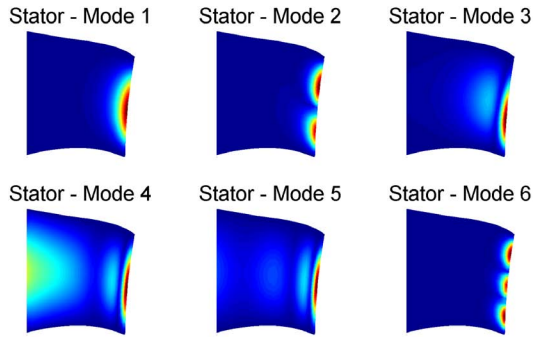


Figure 14. MODE SHAPES FOR ALL BCRs

## Mode Shapes - Rotor

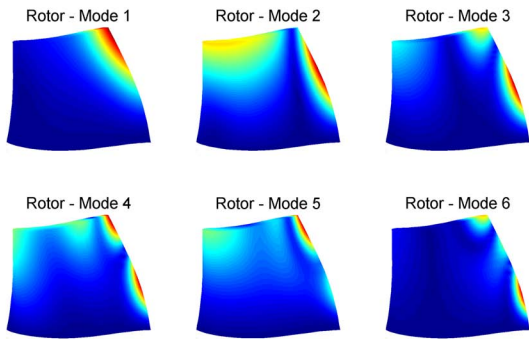


Figure 15. MODE SHAPES OF BCR=1.25

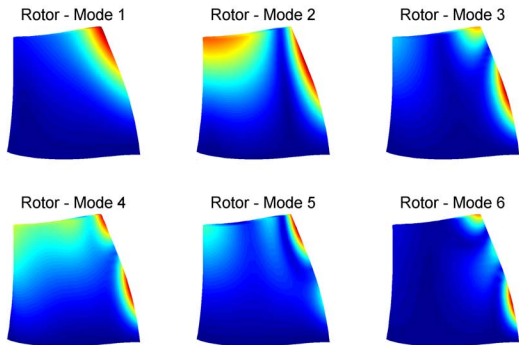


Figure 16. MODE SHAPES OF BCR=1.50

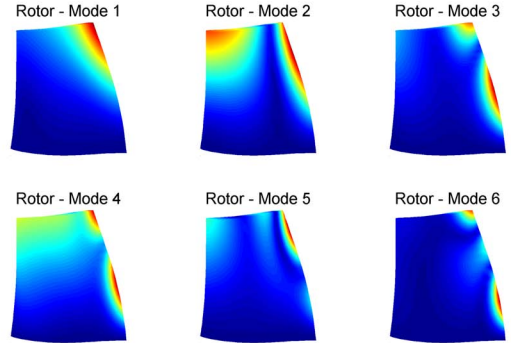


Figure 17. MODE SHAPES OF BCR=1.75

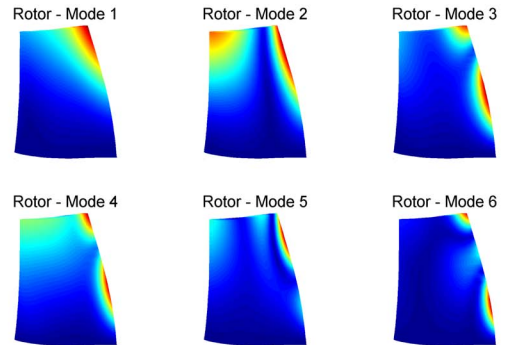


Figure 18. MODE SHAPES OF BCR=2.00

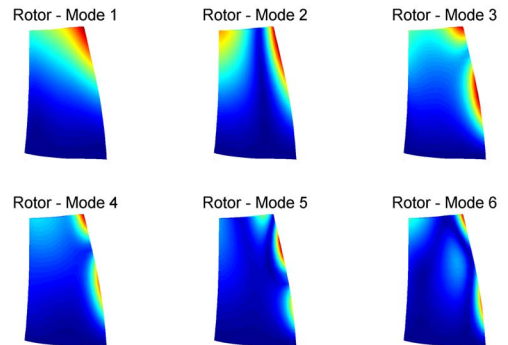


Figure 19. MODE SHAPES OF BCR=2.50

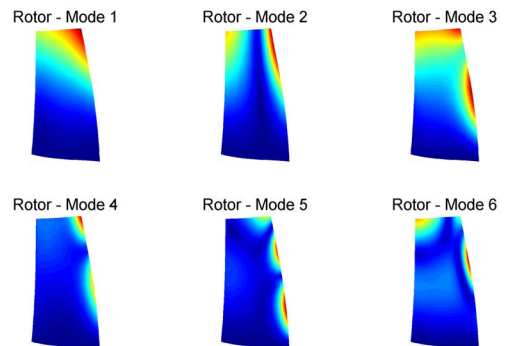


Figure 20. MODE SHAPES OF BCR=3.00